5-Substituted N 4 Hydroxy2'-deoxycytidines and Their 5'-Monophosphates: Synthesis, Conformation, Interaction with Tumor Thymidylate Synthase, and in Vitro Antitumor Activity

ARTICLE *in* JOURNAL OF MEDICINAL CHEMISTRY · NOVEMBER 2000

Impact Factor: 5.45 · DOI: 10.1021/jm000975u · Source: PubMed

5-Substituted N^4-Hydroxy-2′-deoxycytidines and Their 5′-Monophosphates: Synthesis, Conformation, Interaction with Tumor Thymidylate Synthase, and in Vitro Antitumor Activity

Krzysztof Felczak,[†] Agnieszka Miazga,[†] Jarosław Poznański,[†] Maria Bretner,[†] Tadeusz Kulikowski,*[,†] Jolanta M. Dzik,[§] Barbara Gołos,[§] Zbigniew Zieliński,[§] Joanna Cieśla,[§] and Wojciech Rode[§]

Institute of Biochemistry and Biophysics, Polish Academy of Sciences, 5a Pawińskiego Street, 02-106 Warszawa, Poland, and Nencki Institute of Experimental Biology, Polish Academy of Sciences, 3 Pasteur Street, 02-093 Warszawa, Poland

Received May 1, 2000

Convenient procedures are described for the synthesis of 5-substituted N^4-hydroxy-2′-deoxycytidines **5a**,**b**,**d**−**h** via transformation of the respective 5-substituted 3′,5′-di-*O*-acetyl-2′-deoxyuridines **1a**−**c**,**e**−**h**. These procedures involved site-specific triazolation or *N*-methylimidazolation at position C(4), followed by hydroxylamination and deblocking with MeOH−NH_3. Nucleosides **5a**,**b**,**d**−**h** were selectively converted to the corresponding 5′-monophosphates **6a**,**b**,**d**−**h** with the aid of the wheat shoot phosphotransferase system. Conformation of each nucleoside in D_2O solution, deduced from ^{1}H NMR spectra and confirmed by molecular mechanics calculations, showed the pentose ring to exist predominantly in the conformation *S* (C-2′-*endo*) and the N^4-OH group as the *cis* rotamer. Cell growth inhibition was studied with two L5178Y murine leukemia cell lines, parental and 5-fluoro-2′-deoxyuridine (FdUrd)-resistant, the latter 70-fold less sensitive toward FdUrd than the former. With FdUrd-resistant L5178Y cells, 5-fluoro-N^4-hydroxy-2′-deoxycytidine (**5e**) caused almost 3-fold stronger growth inhibition than FdUrd; **5e** was only some 3-fold weaker growth inhibitor of the resistant cells than of the parental cells. Thymidylate synthase inhibition was studied with two forms of the enzyme differing in sensitivities toward 5-fluoro-2′-deoxyuridine 5′-monophosphate (FdUMP), isolated from parental and FdUrd-resistant L1210 cell lines. All N^4-hydroxy-dCMP (**6a**,**b**,**d**−**h**) and dUMP analogues studied were competitive vs dUMP inhibitors of the enzyme. Analogues **6b**,**d**−**h** and 5-hydroxymethyl-dUMP, similar to N^4-hydroxy-dCMP (**6a**) and FdUMP, were also N^5,N^{10}-methylenetetrahydrofolate-dependent, hence mechanism-based, slow-binding inhibitors. 5-Chloro-dUMP, 5-bromo-dUMP, and 5-iodo-dUMP, similar to dTMP, did not cause a time-dependent inactivation of the enzyme. Instead, they behaved as classic inhibitors of tritium release from [5-^{3}H]dUMP. 5-Bromo-dUMP and 5-iodo-dUMP showed substrate activity independent of N^5,N^{10}-methylenetetrahydrofolate in the thymidylate synthase-catalyzed dehalogenation reaction. The ═N−OH substituent of the pyrimidine C(4) prevented the enzyme-catalyzed release from the C(5) of Br^- and I^- (the same shown previously for H^+). While FdUMP and **6a** showed a higher affinity and greater inactivation power with the parental cell than FdUrd-resistant cell enzyme, an opposite relationship could be seen with 5-hydroxymethyl-dUMP.

Introduction

Thymidylate synthase (EC 2.1.1.45) catalyzes the dUMP methylation reaction involving a concerted transfer and reduction of the one-carbon group (at the aldehyde oxidation level) of N^5,N^{10}-methylenetetrahydrofolate, with concomitant production of thymidylate and dihydrofolate.[1,2] Active forms of several drugs used in anticancer, antiviral, and antifungal chemotherapy are thymidylate synthase inhibitors being either dUMP or N^5,N^{10}-methylenetetrahydrofolate analogues.[3−6]

Among the dUMP analogues that are good inhibitors of thymidylate synthase, most involve an electron-withdrawing substituent at the pyrimidine C(5)-position.[7−9] The most prominent example is 5-fluoro-dUMP (FdUMP). Inhibition of thymidylate synthase by FdUMP involves a time-dependent formation of a ternary covalently bound complex of the enzyme with FdUMP and N^5,N^{10}-methylenetetrahydrofolate, in a reaction similar to that with dUMP. However, at this step the reaction stops, as the C(5)-fluorine fails to dissociate (due to the strength of the C−F bond). This results in slowly reversible enzyme inactivation.

A rare example of a dUMP analogue that is C(4)-substituted and, nevertheless, a strong inhibitor of thymidylate synthase,[10] is N^4-hydroxy-2′-deoxycytidine 5′-monophosphate (**6a**). Similar to FdUMP, it is a slow-binding inhibitor, covalently bound by the enzyme, and inactivating it in the presence of N^5,N^{10}-methylenetetrahydrofolate.[10−12] 5-Fluoro substitution in **6a** potentiated inhibition, although in 5-fluoro-N^4-hydroxy-2′-deoxycytidine 5′-monophosphate (**6e**) the N^4-OH substituent probably remained the cause of inactivation.[12]

To pursue those studies, we decided to synthesize a series of new 5-substituted N^4-hydroxy-2′-deoxycytidine

* To whom correspondence should be addressed. Tel/Fax: 48-39-121623. E-mail: tk@ibbrain.ibb.waw.pl.
[†] Institute of Biochemistry and Biophysics.
[§] Nencki Institute of Experimental Biology.

10.1021/jm000975u CCC: $19.00
Published on Web 11/11/2000

5′-phosphates, with different electronic, hydrophobic, and steric properties of their 5-substituents and to compare interactions with thymidylate synthase of those analogues. The nucleoside forms of the analogues were expected to be potential leukemia cell growth inhibitors.

Chemistry

After the observation that hydroxylamine in aqueous solutions reacts selectively with cytosine residues in DNA,[13] N^4-hydroxycytosine (N^4-OH-Cyt) and its analogues were synthesized by direct treatment of cytosine and cytidine with aqueous or anhydrous hydroxylamine, followed by mild acid treatment at an elevated temperature.[14] The reaction is dependent on the addition of hydroxylamine to the 4,5-double bond and replacement of the amino group by hydroxylamine. This led to 4,6-dihydroxylamino derivatives which were converted into the corresponding N^4-hydroxycytosines by acid catalysis at elevated temperature. This reaction was also applied to the preparation of **6a** and dCDP, as well as to hydroxylamination of poly(C).[11,15,16] However, when this procedure was applied to 2′-deoxycytidine, the yield was very poor (16%) due to the substantial deamination and cleavage of glycosidic bond under acidic conditions and elevated temperature.

Better results were obtained by the treatment of 2′-deoxy-3′,5′-di-*O*-benzoyl-4-thiouridine with a methanolic solution of hydroxylamine at reflux temperature to give N^4-hydroxy-2′-deoxycytidine (**5a**) in 48% yield.[17] In the case of 5-fluoro-N^4-hydroxy-2′-deoxycytidine (**5e**) it was advantageous to *S*-methylate 2′-deoxy-5-fluoro-4-thiouridine with diazomethane and to treat the resulting 4-methylthio derivative with hydroxylamine at high dilution. Under these conditions the 4,6-dihydroxylamino derivative was not formed, **5e** being the single product.[18]

Another method of preparation leading to N^4-hydroxycytidines was based on hydroxylamination of the corresponding *O*′-acetylated 4-chlorouridines. However, a four-step procedure and the instability of 4-chloro nucleosides led to poor yields.[19] More recently it was announced that some 2′-deoxyribofuranosyl-4-(1,2,4-triazol-1-yl)pyrimidin-2(1*H*)-ones reacted smoothly with hydroxylamine at room temperature.[20] We decided to apply this modified procedure to the preparation of *O*′-acetylated 5-substituted N^4-hydroxy-2′-deoxycytidines **4a**−**c**,**e**,**f**,**h**.

2′-Deoxy-3′,5′-di-*O*-acetyluridines[21,22] **1a**−**c**,**e**−**h** (Scheme 1) were prepared according to Robins' procedure[23] and subjected to site-specific triazolation[24] at C(4) with triazolide formed from 1,2,4-triazole, $POCl_3$, and TEA. This procedure gave 1,2,4-1*H*-triazolated nucleosides **2a**−**c**,**e**,**f**,**h** in good yield (60−90%).

To improve the yield and to shorten the preparation of **4f**,**g**, we applied the "one-pot" procedure[25] employing *N*-methylimidazolide intermediates, hitherto not used in the synthesis of N^4-hydroxy-2′-deoxy nucleosides, which increased the yield of **3f**,**g** to ca. 80%. The standard deprotection of acetyl groups with MeOH−NH_3 led to the free 5-substituted N^4-hydroxy-2′-deoxycytidines **5a**,**b**,**d**−**h** in ca. 90% yield.

5′-Monophosphates of the N^4-hydroxy-2′-deoxycytidines **6a**,**b**,**d**−**h** were prepared via selective phosphorylation at the 5′-position with the wheat shoot phosphotransferase−4-nitrophenyl phosphate system[26] which gave exclusively 5′-phosphates in 50−70% yields. These compounds proved to be good substrates for snake venom phosphodiesterase (5′-nucleotidase) to give exclusively their mother nucleosides **5a**,**b**,**d**−**h**.

Scheme 1[a]

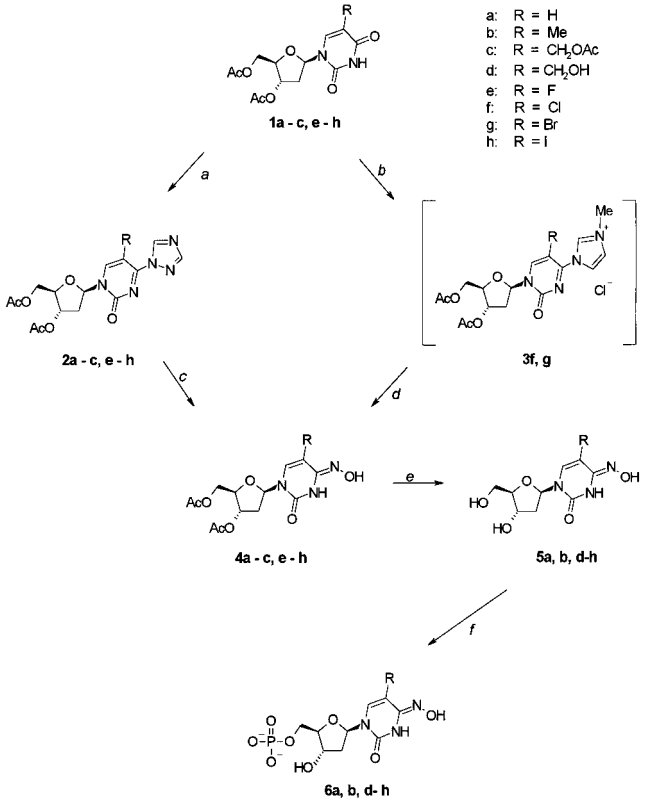

[a] Reagents: (a) 1,2,4-triazole, $POCl_3$, TEA; (b) MeIm, $POCl_3$, Py; (c), (d) NH_2OH; (e) NH_3/MeOH; (f) *p*-nitrophenyl phosphate/wheat shoot phosphotransferase, 37 °C.

Conformational Aspects

Molecular mechanics calculations of a series of C(5)-substituted N^1-methyl-N^4-hydroxycytosines were made with the aid of the Sybyl package. The tripos force field[27] was used with Pullman atomic charges. In the absence of the explicit water molecules the electrostatic interactions were scaled by the distance-dependent dielectric constant $\epsilon = 4.5r$. The initial geometry was adapted from the Sybyl database coordinates of the cytosine. According to quantum mechanical calculations[28] the imino form of the N(4) nitrogen was assumed.

^{1}H NMR spectra of the compounds in neutral aqueous medium (D_2O) were recorded on Varian Unity Plus (500 MHz) spectrometer at 25 °C with the standard program of the solvent signal suppression via presaturation.

The conformational analysis of the deoxyribose moiety was based on ^{1}H NMR spectroscopic data. The seven spin systems were analyzed by the iterative LAOCOON-like[29] program. The sugar ring puckering parameters were estimated from the vicinal ^{1}H−^{1}H coupling constants by Remin interpretation[30] of the algorithm proposed originally by Altona.[31]

Conformation of the N^4-OH Group. Detailed quantum mechanical calculations of Leś et al.[28] demonstrated that in both N^4-hydroxycytosine and its 5-fluoro analogue, the imino form of the N(4) nitrogen was strongly

Table 1. Energy Terms and Structural Details Leading to *Cis* N^4-OH Conformer Stabilization of 5-Substituted N^4-Hydroxy-2′-deoxycytidines

	substituent													
	5-H		5-F		5-Cl		5-Br		5-I		5-Me		5-CH_2OH	
	cis	*trans*	*cis*	*trans*	*cis*	*trans*	*cis*	*trans*	*cis*	*trans*	*cis*	*trans*	*cis*	*trans*
Energy Terms (kcal/mol)														
bond stretching	0.29	0.32	0.28	0.33	0.27	0.42	0.27	0.45	0.27	0.46	0.33	0.67	0.38	0.75
angle bending	1.06	2.18	1.04	2.47	1.05	3.82	1.06	4.24	1.06	4.41	1.28	4.69	1.44	4.93
torsional	0.83	0.71	0.84	0.66	0.84	0.73	0.83	0.74	0.82	0.77	1.64	1.66	1.48	1.54
out of plane	0.02	0.01	0.01	0.00	0.00	0.00	0.00	0.00	0.00	0.00	0.01	0.01	0.02	0.01
1−4 van der Waals	2.51	2.74	2.25	2.45	2.21	2.21	2.18	2.18	2.07	2.22	2.42	2.37	2.92	2.91
van der Waals	−0.48	0.33	−0.56	0.30	−0.71	0.82	−0.76	0.97	−0.83	0.90	−0.52	1.55	−0.44	1.88
1−4 electrostatic	−3.38	−3.45	−1.07	−1.60	−2.23	−2.63	−3.23	−3.43	−3.71	−3.79	−1.65	−2.09	−3.27	−3.60
electrostatic	−0.62	−0.37	−1.01	−0.40	−0.88	−0.41	−0.73	−0.41	−0.64	−0.38	−1.22	−0.72	−0.43	−0.06
total	0.22	2.47	1.78	4.22	0.55	4.96	−0.39	4.75	−0.96	4.58	2.29	8.13	2.09	8.35
trans population estimated at 25 °C	2×10^{-2}		2×10^{-2}		6×10^{-4}		2×10^{-4}		9×10^{-5}		6×10^{-5}		3×10^{-5}	
Geometry (Angles, deg]														
N(3)−C(4)−N(4)	124.1	120.7	123.9	120.4	123.9	119.2	124.0	118.9	124.0	118.9	123.7	118.4	123.7	118.2
C(5)−C(4)−N(4)	118.4	123.9	118.7	124.3	118.7	126.1	118.7	126.6	118.6	126.5	118.3	126.4	118.2	126.6
asymmetry	−5.7	3.2	−5.3	3.9	−5.2	6.9	−5.3	7.7	−5.4	7.6	−5.4	8.0	−5.5	8.3

Chart 1. Rotamers of N^4-Hydroxy-2′-deoxycytidines **5a**,**b**,**d**−**h**

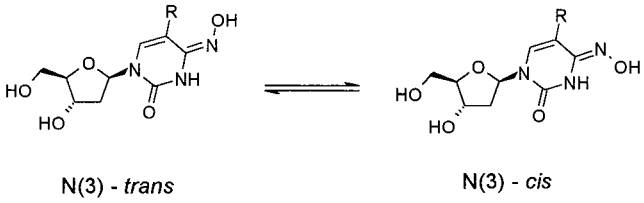

5a: R - H
5b: R - Me
5d: R - CH_2OH
5e: R - F
5f: R - Cl
5g: R - Br
5h: R - I

favored with the oxygen atom lying in the plane of the base. In the case of N^4-hydroxy-2′-deoxycytidine (**5a**), the conformer with the OH group pointed toward the N(3) proton of the base (*cis*) was more stable than the other one, with the hydroxyl pointed toward C(5) (*trans*) (Chart 1). This effect was even more pronounced in the case of 5-fluoro-N^4-hydroxy-2′-deoxycytidine (**5e**).

With all compounds investigated the N^4-OH *cis*−*trans* equilibrium was analyzed by molecular mechanics. The differences of this equilibrium were driven mainly by steric hindrances between the N^4-OH group and the respective C(5)-substituent. The analysis of the energy terms proved that the total stabilization effect mainly resulted from the direct van der Waals interactions as well as from the deformation of the N(3)−C(4)−N(4) and C(5)−C(4)−N(4) angles (cf. van der Waals and angle bending terms in Table 1). In the *trans* conformer the increase of the value of the C(5)−C(4)−N(4) angle accompanied by the decrease of the N(3)−C(4)−N(4) angle resulted in more pronounced separation of the N^4-OH oxygen from the C(5)-substituent. Enlargement of the C(5)-substituent dimension increased the deformation of the *trans* conformation, stabilizing the *cis* one. The deformation was defined by the asymmetry and measured as the difference between the N(3)−C(4)−N(4) and C(5)−C(4)−N(4) angles. For the *cis* conformers the asymmetry value was constant (−5.4 ± 0.2°) and appeared not to be influenced by the C(5)-substituent, whereas for the *trans* conformers the asymmetry value was correlated with the C(5)-substituent's dimensions. In the case of 1-methyl-N^4-hydroxycytosine and its C(5)-fluoro derivative, asymmetry did not exceed 4°. It increased with the increase of the radius of C(5)-substituent up to 8.3° in the case of the hydroxymethyl group. The increase of the asymmetry was not dependent on other, including electrostatic, properties of the C(5)-substituent. An almost linear relation between asymmetry in the *trans* form of the N^4-OH group and the *cis* conformer stabilization energy proved that the C(5)-substituent-induced C(4)−N(4) bond deformation played the main role in destabilization of the *trans* conformation. This led to the sterically driven mechanism of the stabilization of the *cis* conformer of the C(5)-substituted N^4-hydroxy-2′-deoxycytidines. Finally, it may be postulated that apart from **5a**,**e** the population of the *trans* form could be neglected. In fact, NMR spectra of **5a**,**e** proved that both compounds exhibited small populations of the corresponding *trans* conformers (data not presented).

Deoxyribose Conformation. The conformational parameters of the foregoing nucleosides in neutral aqueous medium (D_2O), derived from the vicinal $^1H-^1H$ coupling constants (see Experimental Section) with the aid of the modified Karplus relationship,[31] are listed in Table 2. No significant conformational differences influencing interaction with the enzyme could be found for the sugar ring. For each compound its puckering as well as the population of C(5′)-exocyclic group rotamers are almost identical. The *S* conformer is populated at the level of 0.62 ± 0.02, mean amplitude of pseudorotation, and the population equals 32.8 ± 1.4%, whereas the population of the g^+ rotamer of the C(4′)−C(5′) bond dominates (0.51 ± 0.02).

Biological Results

Cell Growth Inhibition. It was studied with two L5178Y murine leukemia cell lines, parental (L5178Y-P) and 5-fluoro-2′-deoxyuridine resistant (L5178Y-R), the latter 70-fold less sensitive toward FdUrd than the former. Although the resistance mechanism has not been yet fully recognized, preliminary results (not shown), concerning ATP-dependent phosphorylation of

Table 2. Solution Conformation of 5-Substituted N^4-Hydroxy-2′-deoxycytidines in D_2O Calculated from 500-MHz ^1H NMR

	conformation										
compd	S	g^+	t	g^-	Ng^+	Nt	Sg^+	St	Sg^-	F12[a]	F34[a]
5a	0.63	0.47	0.38	0.15	0.23	0.14	0.24	0.24	0.15	1.62	1.00
5b	0.61	0.49	0.36	0.15	0.25	0.14	0.24	0.22	0.15	1.75	1.08
5d	0.64	0.50	0.37	0.13	0.22	0.13	0.27	0.24	0.13	1.67	1.14
5e	0.63	0.53	0.35	0.12	0.24	0.13	0.29	0.22	0.12	1.86	1.32
5f	0.59	0.52	0.29	0.19	0.29	0.12	0.22	0.17	0.19	2.41	1.30
5g	0.61	0.51	0.34	0.15	0.26	0.13	0.25	0.21	0.15	1.93	1.20
5h	0.60	0.53	0.34	0.13	0.26	0.13	0.27	0.21	0.13	1.94	1.31

[a] Lit. ref 30.

Table 3. Inhibition of Growth of L5178Y Parental and FdUrd-Resistant Cells by 5-Substituted 2′-Deoxy Nucleosides and Their N^4-Hydroxy Congeners

	IC_{50}[a] (μM)		
drug	growth assay	[^{14}C]Leu incorp	[^{3}H]Thd incorp
	L5178Y-P		
FdUrd[b]	0.002	0.0024	0.002
CldUrd	32 ± 10 (3)	16 ± 1.4 (3)	33 (1)
BrdUrd	26 ± 2% (2)	20 (1)	26 ± 10% (2)
IdUrd	3.8 ± 4% (2)	4.6 ± 39% (2)	5.4 ± 28% (2)
HmdUrd	6.2 ± 11% (2)		8.6 ± 6% (2)
5a	31 ± 21% (2)		
5e	0.018 ± 0.002 (3)	0.018 ± 3% (2)	0.026 ± 4% (2)
5f	1.15 ± 4% (2)	1.48 ± 6% (2)	1.24 ± 8% (2)
5g	0.98 ± 26% (2)		
5h	32 ± 3% (2)		
5d	4.0 ± 5% (2)		7.0 ± 25% (2)
5b	56 ± 39% (2)		
	L5178Y-R		
FdUrd	0.14 ± 0.01 (3)	0.15 ± 4% (2)	0.13 ± 5% (2)
CldUrd	12 ± 11% (2)		
BrdUrd	12 ± 19% (2)		
IdUrd	2.40 ± 12% (2)		
HmdUrd	11 ± 39% (2)		
5a	193 ± 19% (2)		
5e	0.052 ± 0.005 (3)	0.053 ± 8% (2)	
5f	1.66 ± 2% (2)	3.01 ± 18% (2)	1.03 ± 8% (2)
5g	2.5 ± 61% (2)		
5h	34 ± 23% (2)		
5d	9.1 ± 42% (2)		
5b	163 ± 29% (2)		

[a] IC_{50} is the drug concentration required for 50% reduction in cell number, [^{14}C]Leu incorporation, or [^{3}H]Thd incorporation.[b] Lit. ref 38. [c] Mean ± SEM or mean ± % difference between the mean and each of the two results, followed by the number of experiments (N) in parentheses.

dThd and FdUrd by cell crude extracts, point to altered substrate specificity of this reaction, reflecting presumably thymidine kinase activity, in the resistant cells (with FdUrd being a better substrate than dThd in L5178Y-P but worse than dThd in L5178Y-R cells). None of the nucleoside analogues studied was as strong a growth inhibitor as FdUrd for L5178Y-P cells although 5-fluoro-N^4-hydroxy-2′-deoxycytidine (**5e**) was only about 10-fold weaker (Table 3). Interestingly, with L5178Y-R cells **5e** caused almost 3-fold stronger inhibition than FdUrd. At the same time **5e** was some 3-fold weaker growth inhibitor of the resistant cells than of the parental cells. All other analogues (**5d**−**h**), except for FdUrd and to a smaller extent N^4-hydroxy-2′-deoxycytidine (**5a**) and N^4-hydroxy-5-methyl-2′-deoxycytidine (**5b**), were also rather similarly potent inhibitors of both cell lines. While each 5-chloro-N^4-hydroxy-2′-deoxycytidine (**5f**) and 5-bromo-N^4-hydroxy-2′-deoxycytidine (**5g**) was over 10-fold stronger inhibitor of L5178Y (both parental and FdUrd-resistant) cell growth than the corresponding 5-halogeno-substituted dUrd congener, N^4-hydroxy-5-iodo-2′-deoxycytidine (**5h**) and 5-iodo-2′-deoxyuridine (IdUrd) showed the opposite relation. N^4-Hydroxy-5-hydroxymethyl-2′-deoxycytidine (**5d**) and 5-hydroxymethyl-2′-deoxyuridine (HmdUrd) were similarly potent cell growth inhibitors with each cell line (Table 3).

Thymidylate Synthase-Catalyzed Dehalogenation of 5-Bromo-2′-deoxyuridine 5′-Monophosphate (BrdUMP) and 5-Iodo-2′-deoxyuridine 5′-Monophosphate (IdUMP). With the analogues 5-substituted with chlorine, bromine, or iodine a possibility, their dehalogenation in the thymidylate synthase reaction was tested[32] (see Experimental Section).

With both BrdUMP and IdUMP the absorption maximum changed with time (from 277 to 271 nm for BrdUMP and from 278 to 271 nm for IdUMP). No such changes were visible with CldUMP, N^4-OH-BrdCMP (**6g**), N^4-OH-IdCMP (**6h**), or when the enzyme was omitted. Therefore BrdUMP and IdUMP, but not CldUMP or either 5-halogeno-N^4-hydroxy-2′-deoxycytidine 5′-monophosphate analogue, become dehalogenated by recombinant rat hepatoma thymidylate synthase.

Spectrophotometric monitoring at 338 nm of the dehalogenation reaction mixture, containing either 0.04 mM BrdUMP or 0.04 mM IdUMP, with 0.3 mM methylenetetrahydrofolate demonstrated a slow extinction increase, pointing to dihydrofolate production. The reaction velocity was 20.5 and 34.2 nmol/min·mg protein for BrdUMP and IdUMP, respectively.

Thymidylate Synthase Inhibition by Nucleotides. Thymidylate synthase inhibition was studied with two forms of the enzyme differing in sensitivities toward FdUMP inhibition, isolated from parental and FdUrd-resistant L1210 cell lines.[12] All N^4-OH-dCMP and dUMP analogues studied were competitive vs dUMP inhibitors of the enzyme (Table 4). The 5-substituted N^4-OH-dCMP analogues and HmdUMP, similar to N^4-OH-dCMP (**6a**) and FdUMP, were also N^5,N^{10}-methylenetetrahydrofolate-dependent, hence mechanism-based, slow-binding inhibitors (Table 5). CldUMP, BrdUMP, and IdUMP, similar to dTMP, did not cause time-dependent inactivation of the enzyme. Instead, they behaved as classic inhibitors of tritium release from [5-^{3}H]dUMP, in agreement with substrate activity of BrdUMP and IdUMP in the dehalogenation reaction (see above) and CldUMP being a classic inhibitor.

While previously studied FdUMP and N^4-OH-dCMP (**6a**) showed higher affinity (Table 4) and greater inactivation power (Table 3) with the parental cell than a FdUrd-resistant cell enzyme, a definitely opposite relationship could be seen with HmdUMP (Tables 4 and 5).

Table 4. Parameters Describing Time-Independent Inhibition of Thymidylate Synthase from L1210 Parental and FdUrd-Resistant Cells by 5-Substituted N^4-Hydroxy-2′-deoxycytidine 5′-Monophosphates and dUMP Analogues

	L1210-P enzyme		L1210-R enzyme	
compd	K_i (μM)	K_i/K_m	K_i (μM)	K_i/K_m
6a[a]	1.7	0.68	9.3	5.5
FdUMP[a]	0.02	0.008	0.03	0.018
6e[a]	0.8	0.32	1.4	0.82
CldUMP	0.3	0.12	0.15	0.088
6f	8.5	3.4	8.4	4.9
BrdUMP	1.5	0.6	0.46	0.27
6g	32.1	13	36.6	22
IdUMP	7.68	3.1	6.99	4.1
6h	7.46	3	5.7	3.4
HmdUMP	3.7	1.5	0.9	0.53
6d	1.91	0.76	2.18	1.3
dTMP	7.3	2.9		

[a] Lit. ref 12.

Discussion

Cell Growth Inhibition. The parent N^4-OH-dCyd (**5a**) has been previously demonstrated as a L5178Y and Burkitt's lymphoma cell growth inhibitor with IC_{50} values of 12 μM[33] and 1.7−4.0 μM,[34] respectively. In our hands it was some 3-fold weaker inhibitor of L5178Y-P cell growth (Table 3). However, the 5-fluoro substituent, in N^4-OH-FdCyd (**5e**), potentiated inhibition of cell growth almost 2000-fold (Table 3), whereas with Burkitt's lymphoma cells the corresponding effect amounted to 60-fold, IC_{50} value for **5e** being 0.027 μM.[34] Potentiation of L5178Y cell growth inhibition by a 5-substituent at N^4-OH-dCyd (**5a**) was apparent also with N^4-OH-CldCyd (**5f**), N^4-OH-BrdCyd (**5g**), and N^4-OH-HmdCyd (**5d**) but not with N^4-OH-IdCyd (**5h**) or N^4-OH-MedCyd (**5b**) (Table 3). Combinations of the C(4)═N−OH with either C(5)-Cl in **5f** or C(5)-Br in **5g** resulted clearly in a synergistic effect on inhibition of both cell lines, reflected by lower IC_{50} values for each combination than for each of the corresponding singly substituted congeners (Table 3).

N^4-OH-dCyd (**5a**)[33,34] and its 5-fluoro congener N^4-OH-FdCyd (**5e**)[34] have been shown to be thymidine and deoxyuridine, rather than deoxycytidine, antimetabolites. An elaborated study demonstrated N^4-OH-dCyd (**5a**) to be phosphorylated in L5178Y cells to the 5′-monophosphate, in an ATP-dependent reaction inhibited by thymidine and deoxyuridine, but not deoxycytidine, and as the monophosphate to inhibit thymidylate synthase.[33] That is why it was interesting to compare the effect of N^4-OH-dCyd (**5a**) and its analogues on two cell lines differing in sensitivity to another thymidine and deoxyuridine antimetabolite, FdUrd, also phosphorylated to the monophosphate and targeted at the same enzyme. [2−4] Interestingly, while both N^4-OH-dCyd (**5a**) and its 5-fluoro congener N^4-OH-FdCyd (**5e**) were severalfold weaker inhibitors of L5178Y-R (FdUrd-resistant) than L5178Y-P (parental) cells, combination of the C(4)═N−OH with C(5)-F substituents in N^4-OH-FdCyd (**5e**) resulted in stronger inhibition of the resistant line than that caused by FdUrd (although the latter inhibited the parental line 9-fold stronger than **5e**). One possible suggestion of an explanation is apparently altered substrate specificity of nucleoside phosphorylation in the resistant cells (see above), but further studies of the resistance mechanism are needed to clarify this point.

Interaction with Enzyme. Dehalogenation of BrdUMP and IdUMP by bacterial thymidylate synthase from *Lactobacillus casei* has been previously described.[32] Lack of dehalogenation of the corresponding derivatives of N^4-OH-dCMP (**6a**) is similar to the earlier demonstrated lack of C(5)-proton release from **6a** in thymidylate synthase-catalyzed reaction.[12] The latter result has been interpreted in terms of the C(4)═N−OH, probably interacting with N^5,N^{10}-methylenetetrahydrofolate, being the cause of the reaction arrest at a step preceding release of H^+ from C(5). Such an explanation has been further supported by molecular modeling studies.[2,35] Considering lack of dependence of the dehalogenation reactions (with BrdUMP and IdUMP) on N^5,N^{10}-methylenetetrahydrofolate, failure of the enzyme to release Br^- or I^- from **6g** or **6h** in the absence of the cofactor suggests an influence of the C(4)═N−OH on the C(5)−Br and C(5)−I bonds, rendering the corresponding halogen anion release impossible. Hence, the ═N−OH substituent at the pyrimidine C(4) appears to provide both BrdUMP and IdUMP with potency to inactivate the enzyme. This also concerns CldUMP, although it shows no thymidylate synthase-catalyzed dehalogenation in agreement with previous results,[32] which ap-

Table 5. Parameters[b] for Time-Dependent Inactivation, Reflecting Slow-Binding Inhibition, by FdUMP and 5-Substituted N^4-Hydroxy-2′-deoxycytidine 5′-Monophosphates of Thymidylate Synthase from L1210 Parental and FdUrd-Resistant Cells

compd	enzyme source	K_i' (μM)	K_i'' (μM)	k_2' (min^{-1})	k_2'' (min^{-1})
FdUMP[a]	L1210-P	0.0018	0.02	0.17	0.12
FdUMP[a]	L1210-R	0.0122	0.014	0.25	0.06
6a[a]	L1210-P	0.063	0.226	0.17	0.02
6a[a]	L1210-R	0.184	1.46	0.20	0.09
6e[a]	L1210-P	0.073	0.056	0.24	0.07
6e[a]	L1210-R	0.093	0.071	0.24	0.06
6f	L1210-P	20 ± 2 (3)	16 ± 2 (3)	0.17 ± 0.01 (3)	0.06 ± 0.00 (3)
6f	L1210-R	31 ± 9 (3)	15 ± 6 (3)	0.19 ± 0.03 (3)	0.06 ± 0.02 (3)
6g	L1210-P	33 ± 8 (3)	26 ± 3 (3)	0.23 ± 0.05 (3)	0.07 ± 0.01 (3)
6g	L1210-R	36 ± 5 (3)	11 ± 1 (3)	0.22 ± 0.03 (5)	0.05 ± 0.01 (5)
6h	L1210-P	4.9 ± 1.1 (3)	14 ± 2 (3)	0.21 ± 0.01 (3)	0.02 ± 0.00 (3)
6h	L1210-R	4.2 ± 1.9 (3)	8.6 ± 1.2 (3)	0.30 ± 0.03 (3)	0.11 ± 0.03 (3)
HmdUMP	L1210-P	57 ± 18 (3)	16 ± 2 (3)	0.74 ± 0.09 (3)	0.02 ± 0.00
HmdUMP	L1210-R	17 ± 1 (3)	9.9 ± 3.0 (3)	0.63 ± 0.01 (3)	0.02 ± 0.01
6d	L1210-P	3.8 ± 1.1 (3)	4.7 ± 1.3 (3)	0.45 ± 0.09 (3)	0.23 ± 0.06 (3)
6d	L1210-R	5.7 ± 1.1 (3)	1.4 ± 0.3 (3)	0.72 ± 0.17 (3)	0.15 ± 0.02 (3)

[a] Lit. ref 12. [b] Mean ± SEM or mean ± % difference between the mean and each of the two results, followed by the number of experiments (N) in parentheses.

pears to be only a classic inhibitor of the enzyme. However, with the =N−OH substituent at the pyrimidine C(4) it becomes a slow-binding inhibitor.

In view of the results of the preliminary QSAR study of the 5-substituted dUMP analogues,[36] a large steric effect causes weaker interaction with thymidylate synthase by IdUMP, as compared with other 5-halogenated congeners. However, comparison of enzyme inhibition by the 5-halogenated analogues of **6a** shows an interesting departure from this relationship, reflected by a stronger inhibition, particularly of the slow-binding type, caused by N^4-OH-IdCMP (**6h**) than N^4-OH-BrdCMP (**6g**) or N^4-OH-CldCMP (**6f**) (Tables 4 and 5). The latter suggests an interplay between the substituents at C(4) and C(5) in **6h** interacting with thymidylate synthase. A similar interplay between the C(4)=N−OH and C(5)-F substituents in N^4-OH-FdCMP (**6e**) was indicated by our previous results.[12] To explain it, an intramolecular hydrogen bond $=N^4-OH\cdots F-C(5)$ was hypothesized, influencing an assumed *cis*−*trans* equilibrium of rotamers, resulting in stabilization of the rare species *trans*, found to be the only inhibitory form.[12] However our present results, based on molecular mechanics calculations (Table 1), bring into question the $=N^4-OH\cdots F-C(5)$ hydrogen bond formation as a main factor of stabilization of the *trans* species (cf. ref 28). The compounds exhibiting lowered population of the rare *trans* conformer, caused by the unfavorable O^4-C(5)-substituent steric interaction (such as in **6b**,**e**−**h**), show significantly lower inhibitory activity against thymidylate synthase than either **6a** or **6e**.

Conclusions

The most convenient procedures for the synthesis of 5-substituted N^4-hydroxy-2′-deoxycytidines **5a**,**b**,**d**−**h** involve site-specific triazolation or *N*-methylimidazolation of the respective 5-substituted 3′,5′-di-*O*-acetyl-2′-deoxyuridines followed by hydroxylamination and deblocking with $MeOH-NH_3$.

Steric interaction between the 5-substituent and the N(4)-oxygen strongly destabilizes the *trans* conformation of the N^4-OH group when the van der Waals radius of the substituent exceeds 1D.

The =N−OH substituent at the pyrimidine C(4) provides **6a** and its analogues with potency to inactivate thymidylate synthase. Inactivation depends on the population of the rare *trans* conformer (with the N^4-OH pointed toward the C(5)); hence compounds exhibiting lowered population of the *trans* conformer, caused by an unfavorable O^4-C(5)-substituent steric interaction, are weaker slow-binding inhibitors of the enzyme than **6a** or its 5-fluoro congener.

The =N−OH substituent of the pyrimidine nucleotide C(4) prevents the enzyme-catalyzed release of Br^- and I^- from the C(5) (the same shown previously for H^+). **5e** shows a strong cell growth inhibitory activity against FdUrd-resistant tumor cells.

Experimental Section

General Methods. Melting points (uncorrected) were measured on a Boetius microscopic hot stage; UV spectra were recorded on a Cary 300 instrument, using 10-mm path length cuvettes. Extremes of pH made use of standard solutions of HCl and NaOH. A phosphate buffer was used (pH 7.00). A Cole-Parmer instrument with combination electrode was employed for pH measurements. Liquid matrix secondary ion mass spectra (LSIMS) were recorded for nucleosides with an AMD-604 spectrometer. High-resolution ^{1}H NMR spectra were recorded on a Varian 500 MHz in D_2O with DSS as internal standard or in $CDCl_3$ with tetramethylsilane as internal standard. Thin-layer chromatography (TLC) was run on Merck silica gel F_{254} glass plates (DC, 20 × 20 cm, 0.25 mm; no. 1.05715) and Merck cellulose F glass plates (DC, 20 × 20 cm, 0.1 mm; no. 1.05718). Preparative-layer chromatography (PLC) was run on Merck silica gel F_{254} glass plates (PLC, 20 × 20 cm, 2 mm; no. 1.05717). The following solvents (v/v) were used: (A) $CHCl_3$−MeOH, 80:20; (B) $CHCl_3$−MeOH, 95:5; (C) *i*-PrOH−EtOAc−toluene, 10:20:70; (D) MeOH−concentrated aqueous NH_3-H_2O, 70:10:20; (E) EtOH−1 M CH_3COONH_4, 70:50; (F) saturated aqueous $(NH_4)_2SO_4$−0.05 M phosphate buffer pH 6−*i*-PrOH, 79:19:2; DEAE-Sephadex A-25 was purchased from Pharmacia. Relation of phosphorus/extinction (P/ϵ) was determined using micromethod of Chen, Toribara and Warner.[37]

Cell Lines. Mouse leukemia L5178Y cells were grown as reported earlier.[38] The FdUrd-resistant cell line was developed by growing in the presence of the drug in the cell medium. FdUrd concentration was increased (stepwise and always after cells became adapted to the previous concentration) up to 0.1 μM.

In Vitro Cell Growth Inhibition. The influence of each analogue on viability of exponentially growing cells and [^{14}C]-leucine and [^{3}H]thymidine incorporation was followed, and IC_{50} values were determined as previously described.[38]

Thymidylate Synthase. Highly purified preparations of thymidylate synthase, differing in sensitivity to FdUMP slow-binding inhibition, from parental and FdUrd-resistant L1210 cells,[12,39] as well as the pure recombinant rat hepatoma enzyme[40] have been described in more detail elsewhere. The [5-^{3}H]dUMP tritium release activity assay was performed as previously described.[12] The dUMP and dCMP analogues were added to the reaction mixtures as neutral aqueous solutions. Reaction mixtures and procedures used in inhibition studies were as earlier described.[12,41]

Thymidylate Synthase-Catalyzed Dehalogenation of dUMP Analogues. Highly purified recombinant rat hepatoma thymidylate synthase (specific activity 0.6 μmol/min/mg protein at 30 °C) was used.[12,40] The reaction mixture contained 50 mM *N*-methylmorpholine-HCl pH 7.4, 6.5 mM DTT, 25 mM $MgCl_2$, 1 mM EDTA, one of the nucleotide analogues (0.042 mM 5-chloro-2′-deoxyuridine 5′-monophosphate (CldUMP), 0.04 mM BrdUMP, 0.038 mM IdUMP, 0.043 mM **6g** or 0.043 mM **6h**) and the enzyme (0.004 mM) in a total volume of 0.42 mL. Samples were incubated at 30 °C and UV spectra were monitored in the course of 120 min using Beckman DU-64 spectrophotometer.

Kinetic Studies. To identify the type of inhibition involved, the effects of the **6a** analogues on the dependence of reaction rate on dUMP concentration, in the form of Liveweaver−Burk plots, were analyzed as previously reported with the use of a program, based on nonlinear regression and designed for estimation of kinetic constants describing competitive (both linear and parabolic), noncompetitive, uncompetitive, or mixed-type linear inhibition.[41]

Quantitative analyses of thymidylate synthase inhibition by 5-substituted N^4-OH-dCMP analogues or HmdUMP leading to time-dependent inactivation of the enzyme were performed by following the decrease of enzyme activity with time (usually at 0.5, 1.0, 1.5, 4, 6, 8 and 10 min) during preincubation of the enzyme at 37 °C in the presence of 0.8 mM (6*RS*,a*S*)-CH_2H_4PteGlu, 3.3 μM dUMP (to prevent thermal inactivation), and various concentrations of inhibitor. Activity remaining after preincubation was determined by addition of 25 μM [5-^{3}H]dUMP (7×10^4 dpm/nmol) and tritium release after 4 min incubation was measured. The slopes of the semilog plots of percent (%) remaining activity vs preincubation time, expressing apparent inactivation rate constants (k_{app}) and corresponding inhibitor concentrations [*I*], were then replotted as double-reciprocal plots, according to the relationship:[41]

$$\frac{1}{k_{app}} = \left(\frac{K_i[S]}{K_m k_2} + \frac{K_i}{k_2}\right)\frac{1}{[I]} + \frac{1}{k_2}$$

where k_2 is the inactivation rate constant. The values of k_2 and K_i were determined from the plot intercept and slope, respectively.[38,42]

Statistically Evaluated Results. These are presented as means ± SEM or means ± percent difference between the mean and each of the two results, followed by the number of experiments (*N*) in parentheses.

General Procedure for the Synthesis of 1,2,4-Triazole 5-Substituted 3′,5′-Di-*O*-acetyl-2′-deoxyuridines 2a−c,e,f,h. 1,2,4-Triazole (625 mg, 9.05 mmol) was suspended in MeCN (5 mL) at 0 °C, phosphoryl chloride (180 μL, 1.93 mmol) was added over 2 min and the mixture was stirred at 0 °C for 10 min. After addition of triethylamine (1.2 mL, 8.61 mmol) over 5 min the mixture was stirred at 0 °C for a further 20 min. 3′,5′-Di-*O*-acetyl derivative of the appropriate 2′-deoxy nucleoside (**1a**−**c**,**e**,**f**,**h**)[21−24] (1 mmol) in MeCN (5 mL) was added and the solution stirred at room temperature overnight. Triethylamine (820 μL, 5.93 mmol) and water (215 μL, 11.94 mmol) were then added and after 10 min the solvents were evaporated under reduced pressure. The residue was partitioned between $CHCl_3$ (35 mL) and saturated aqueous $NaHCO_3$. The organic layer was dried (Na_2SO_4) and evaporated. The crude products were purified as follows.

1-(3,5-Di-*O*-acetyl-*β*-D-2-deoxyribofuranosyl)-4-(1,2,4-triazol-1-yl)pyrimidin-2(1*H*)-one (2a). Crude product was crystallized from MeOH to yield white crystals: 330 mg (91%); mp 150−153 °C; UV λ_{max} (MeOH) 312 nm (ϵ 8.1 × 10^3), 248.5 nm (ϵ 13.5 × 10^3), 214.5 (ϵ 17.35 × 10^3); TLC (silica gel) R_f (C) 0.18; ^{1}H NMR δ ($CDCl_3$) 9.27, 8.13 (2H, 2 × s, 2 × triazolo CH), 8.28 (1H, d, H5), 7.10 (1H, d, H6), 6.27 (1H, dd, H1′), 5.25−5.23 (1H, m, H3′), 4.42−4.40 (2H, m, H5′, H5″), 2.95 (1H, m, H4′), 2.13, 2.09 (6H, 2 × s, 2 × CH_3CO), 2.20−2.08 (2H, m, H2′, H2″).

1-(3,5-Di-*O*-acetyl-*β*-D-2-deoxyribofuranosyl)-4-(1,2,4-triazol-1-yl)-5-methylpyrimidin-2(1*H*)-one (2b). The product was crystallized from MeOH to yield white crystals: 351 mg (93%); mp 126−131 °C (lit.[43] 120−122 °C); UV λ_{max} (MeOH) 326.5 nm (ϵ 7.8 × 10^3), 249.5 nm (ϵ 10.3 × 10^3), 215.5 nm (ϵ 18.2 × 10^3); TLC (silica gel) R_f (C) 0.18.

1-(3,5-Di-*O*-acetyl-*β*-D-2-deoxyribofuranosyl)-4-(1,2,4-triazol-1-yl)-5-fluoropyrimidin-2(1*H*)-one (2e). Crude compound **2e**, homogeneous on TLC (silica gel) R_f (B) 0.75, was used in the next step without further purification.

1-(3,5-Di-*O*-acetyl-*β*-D-2-deoxyribofuranosyl)-4-(1,2,4-triazol-1-yl)-5-chloropyrimidin-2(1*H*)-one (2f). Crude product was chromatographed on a silica gel column (1 × 30 cm) with $CHCl_3$ as eluent to give a foam. Crystallization from MeOH yielded white crystals: 290 mg (73%); mp 140−145 °C; UV λ_{max} (MeOH) 332.5 nm, 249 nm; TLC (silica gel) R_f (C) 0.25; ^{1}H NMR δ ($CDCl_3$) 9.20, 8.20 (2H, 2 × s, 2 × triazolo CH), 8.45 (1H, d, H6), 6.26 (1H, dd, H1′), 5.26−5.22 (1H, m, H3′), 4.46−4.42 (3H, m, H4′, H5′, H5″), 2.95−2.89 (1H, m, H2″), 2.27−2.20 (1H, m, H2′), 2.18, 2.15 (6H, 2 × s, 2 × CH_3CO); MS *m*/*z* 398.08470 [(M + H)$^+$, calcd for $C_{15}H_{17}O_6N_5{}^{35}Cl$ 398.08674].

1-(3,5-Di-*O*-acetyl-*β*-D-2-deoxyribofuranosyl)-4-(1,2,4-triazol-1-yl)-5-iodopyrimidin-2(1*H*)-one (2h). Crude compound **2h**, homogeneous on TLC (silica gel) R_f (C) 0.30, was used in the next step without further purification.

1-(3,5-Di-*O*-acetyl-*β*-D-2-deoxyribofuranosyl)-4-hydroxyaminopyrimidin-2(1*H*)-one (4a). 200 mg (0.55 mmol) of 1-(3,5-di-*O*-acetyl-*β*-D-2-deoxyribofuranosyl)-4-(1,2,4-triazol-1-yl)pyrimidin-2(1*H*)-one (**2a**) was dissolved in 20 mL of pyridine and hydroxylamine hydrochloride (150 mg, 2.16 mmol) was added. The mixture was stirred at room temperature for 12 h, evaporated under reduced pressure and coevaporated successively with 2 × 20 mL of toluene and EtOH. 50 mL of $CHCl_3$ was added and the mixture was washed with water (2 × 30 mL). The organic layer was dried (Na_2SO_4), evaporated under reduced pressure and crystallized from the mixture of toluene and MeOH to yield white crystals: 154 mg (86%); mp 177−184 °C; UV λ_{max} (pH 0) 280 nm (ϵ 10.4 × 10^3), 219 nm (ϵ 6.9 × 10^3); λ_{max} (pH 1) 279.5 nm (ϵ 10.2 × 10^3), 220 nm (ϵ 7.0 × 10^3); λ_{max} (pH 2) 278.5 nm (ϵ 8.7 × 10^3), 224 nm (ϵ 6.9 × 10^3); λ_{max} (pH 7) 270 nm (ϵ 5.2 × 10^3), 234 nm (ϵ 10.0 × 10^3); λ_{max} (pH 12) 240 nm (ϵ 8.2 × 10^3); TLC (silica gel) R_f (C) 0.21; ^{1}H NMR δ ($CDCl_3$) 6.80 (1H, d, H5), 6.30 (1H, dd, H1′), 5.65 (1H, d H6), 5.19−5.18 (1H, m, H3′), 4.34−4.28 (2H, m, H5′, H5″), 4.20 (1H, m, H4′), 2.38−2.35 (1H, m, H2″), 2.17−2.14 (1H, m, H2′), 2.11, 2.10 (6H, 2 × s, 2 × CH_3CO). Anal. ($C_{13}H_{17}N_3O_7$·0.5MeOH) C, H, N.

1-(3,5-Di-*O*-acetyl-*β*-D-2-deoxyribofuranosyl)-4-hydroxyamino-5-methylpyrimidin-2(1*H*)-one (4b). 200 mg (0.53 mmol) of 1-(3,5-di-*O*-acetyl-*β*-D-2-deoxyribofuranosyl)-4-(1,2,4-triazol-1-yl)-5-methylpyrimidin-2(1*H*)-one (**2b**) was dissolved in 10 mL of pyridine and hydroxylamine hydrochloride (150 mg, 2.16 mmol) was added. The mixture was stirred at room temperature for 12 h, evaporated under reduced pressure and coevaporated successively with 2 × 20 mL of toluene and EtOH. 50 mL of $CHCl_3$ was added and the mixture was washed with water (2 × 30 mL). The organic layer was dried (Na_2SO_4), evaporated under reduced pressure and crystallized from MeOH to yield white crystals: 145 mg (80%); mp 140−143 °C; UV λ_{max} (pH 0) 285 nm (ϵ 13.60 × 10^3), λ_{max} 220 nm (ϵ 9.60 × 10^3) λ_{max} (pH 1) 282.5 nm (ϵ 12.40 × 10^3), λ_{max} 220 nm (ϵ 9.00 × 10^3), λ_{max} (pH 2) 278 nm (ϵ 9.90 × 10^3), λ_{max} 224 nm (ϵ 9.40 × 10^3), λ_{max} (pH 7) 268 nm (ϵ 8.60 × 10^3), λ_{max} 236 nm (ϵ 11.55 × 10^3) λ_{max} (pH 12) 252 nm (ϵ 10.80 × 10^3); TLC (silica gel) R_f (C) 0.32; ^{1}H NMR δ ($CDCl_3$) 6.34 (1H, dd, H1′), 6.11 (1H, d, H6), 5.21−5.18 (1H, m, H3′), 4.36−4.30 (2H, m, H5′, H5″), 4.20−4.18 (1H, m, H4′), 2.35−2.30 (1H, m, H2″), 2.19−2.13 (1H, m, H2′), 2.14, 2.11 (6H, 2 × s, 2 × CH_3CO), 1.83 (3H, s, CH_3. Anal. ($C_{14}H_{19}N_3O_7$·1.5H_2O) C, H, N.

1-(3,5-Di-*O*-acetyl-*β*-D-2-deoxyribofuranosyl)-4-hydroxyamino-5-acetoxymethylpyrimidin-2(1*H*)-one (4c). 5-Hydroxymethyl-2′-deoxyuridine[44] 258 mg (1 mmol), 6 mL of Ac_2O and 7.5 mg of DMAP were stirred at room temperature for 24 h. At this point TLC (solvent C) indicated the completion of the reaction. The reaction mixture was evaporated to dryness in vacuo and evaporated twice with EtOH. Chromatographically homogeneous residue (385 mg) was directly used in triazolation reaction, to give crude **2c** which was used in the preparation of **4c**. 200 mg (0.46 mmol) of 1-(3,5-di-*O*-acetyl-*β*-D-2-deoxyribofuranosyl)-4-(1,2,4-triazol-1-yl)-5-acetoxymethylpyrimidin-2(1*H*)-one (**2c**) was dissolved in 20 mL of pyridine and hydroxylamine hydrochloride (150 mg, 2.16 mmol) was added. The mixture was stirred at room temperature for 12 h, evaporated under reduced pressure and coevaporated successively with 2 × 20 mL of toluene and EtOH. 50 mL of $CHCl_3$ was added and the mixture was washed with water (2 × 30 mL). The organic layer was dried (Na_2SO_4) and evaporated under reduced pressure. The residue was crystallized from a mixture of toluene and MeOH to yield white crystals: 167 mg (91%); mp 122−125 °C; UV λ_{max} (pH 0) 281.5 nm (ϵ 14.20 × 10^3), λ_{max} 219 (ϵ 12.40 × 10^3); λ_{max} (pH 1) 281.5 nm (ϵ 9.60 × 10^3), λ_{max} 224.5 nm (ϵ 8.80 × 10^3); λ_{max} (pH 2) 275 nm (ϵ 7.60 × 10^3), λ_{max} 230 nm (ϵ 12.10 × 10^3); λ_{max} (pH 7) 274 nm (ϵ 6.90 × 10^3), λ_{max} 231.5 nm (ϵ 12.75 × 10^3); λ_{max} (pH 12) 251 nm (ϵ 10.60 × 10^3); TLC (silica gel) R_f (C) 0.33; ^{1}H NMR δ ($CDCl_3$) 7.03 (1H, s, H6), 6.30 (1H, dd, H1′), 5.21 (1H, m, H3′), 4.82−4.70 (2H, dd, CH_2OH), 4.36 (1H, dd, H5″), 4.30 (1H, dd, H5′), 4.21 (1H, m, H4′), 2.39−2.34 (1H, m, H2″), 2.20−2.05 (1H, m, H2′), 2.17, 2.11, 2.07 (9H, 3 × s, 3 × CH_3CO). Anal. ($C_{16}H_{21}N_3O_9$·0.33MeOH) C, H, N.

1-(3,5-Di-*O*-acetyl-*β*-D-2-deoxyribofuranosyl)-4-hydroxyamino-5-fluoropyrimidin-2(1*H*)-one (4e). To the solution of 332 mg (0.87 mmol) of 2′-deoxy-3′,5′-di-*O*-acetyl-5-fluoro-4-triazolouridine (**2e**) in 10 mL of MeOH were added 530 mg (6.6 mmol) of NH_2OH × HCl dissolved in 10 mL of MeOH and sodium methoxide prepared by dissolving of 152 mg (6.6 mmol) of Na in 5 mL of MeOH. The solution was stirred at room temperature and progress of the reaction was monitored by TLC on silica gel in solvent B. After completion of the reaction (ca. 1 h) the mixture was concentrated under reduced pressure, dissolved in water and extracted with $CHCl_3$. The organic layer

was dried (Na_2SO_4) and evaporated, the residue crystallized from EtOH to yield white crystals 220 mg. The mother liquors were purified on a preparative silica gel plate developed in solvent B. Products were combined to yield colorless crystals: 276 mg (92%); mp 162−163 °C; UV λ_{max} (pH 0) 286 nm (ϵ 14.6 × 10^3), 222 nm (ϵ 10.6 × 10^3); λ_{max} (pH 2) 270 nm (ϵ 9.7 × 10^3), 234 nm (ϵ 12.2 × 10^3); λ_{max} (pH 7) 270 nm (ϵ 10.4 × 10^3), 234 nm (ϵ 13.3 × 10^3); λ_{max} (pH 12) 253 nm (ϵ 13.5 × 10^3); TLC (silica gel) R_f (C) 0.37. Anal. ($C_{13}H_{16}FN_3O_7$) C, H, N.

1-(3,5-Di-*O*-acetyl-*β*-D-2-deoxyribofuranosyl)-4-hydroxyamino-5-chloropyrimidin-2(1*H*)-one (4f). 1.06 g (3 mmol) of 1-(3,5-di-*O*-acetyl-*β*-D-2-deoxyribofuranosyl)-5-chlorouracil (**1f**) was dissolved in 15 mL of dry MeCN and added to *N*-methylphosphoimidazolide prepared from 2.4 mL (30 mmol) of *N*-methylimidazole and 840 μL (9 mmol) $POCl_3$ in 60 mL of MeCN. The mixture was stirred for 2h at room temperature and 9.5 mmol of hydroxylamine in 10 mL of MeOH was added. Stirring was continued for 2 h at room temperature and reaction mixture was evaporated to dryness in vacuo. The residue was dissolved in 20 mL of water and extracted (3 × 50 mL) with EtOAc. The extract was washed with 30 mL water, dried over $MgSO_4$, evaporated to dryness in vacuo to give ca. 1 g of crude product, which was dissolved in MeOH and deposited on Dowex 50W(H^+) column (1.5 × 20 cm) and eluted with a gradient of TEA in MeOH (0−1 M). The fractions containing **4f** were concentrated under vacuum and crystallized from EtOH to yield white crystals: 850 mg (78%); mp 178−180 °C; UV λ_{max} (pH 0) 294 nm (ϵ 15.3 × 10^3), 226 nm (ϵ 11.9 × 10^3); λ_{max} (pH 1) 288 nm (ϵ 10.8 × 10^3), 226 nm (ϵ 12.4 × 10^3); λ_{max} (pH 2) 282 nm (ϵ 10.2 × 10^3), 233 nm (ϵ 13.2 × 10^3); λ_{max} (pH 7) 281 nm (ϵ 10.1 × 10^3), 234 nm (ϵ 13.8 × 10^3); λ_{max} (pH 12) 284 nm (ϵ 9.4 × 10^3), 250 nm (ϵ 14.2 × 10^3); TLC (silica gel) R_f (C) 0.41; ^{1}H NMR δ ($CDCl_3$) 7.13 (1H, s, H6), 6.34 (1H, dd, H1′), 5.23−5.20 (1H, m, H3′), 4.37 (1H, dd, H5″), 4.32 (1H, dd, H5′), 4.24−4.22 (1H, m, H4′), 2.42−2.38 (1H, m, H2″), 2.19−2.12 (1H, m, H2′), 2.18, 2.11 (6H, 2 × s, 2 × CH_3CO). Anal. ($C_{13}H_{16}ClN_3O_7$) C, H, N.

1-(3,5-Di-*O*-acetyl-*β*-D-2-deoxyribofuranosyl)-4-hydroxyamino-5-bromopyrimidin-2(1*H*)-one (4g). 1.28 g (3 mmol) of 1-(3,5-di-*O*-acetyl-*β*-D-2-deoxyribofuranosyl)-5-bromouracil (**1g**) was dissolved in 15 mL of dry MeCN and added to the *N*-methylphosphoimidazolide prepared from 2.4 mL (30 mmol) of *N*-methylimidazole and 840 μL (9 mmol) $POCl_3$ in 60 mL of MeCN. The mixture was stirred for 2 h at room temperature to give intermediate **3g** and 9.5 mmol of hydroxylamine in 10 mL of MeOH was added. Stirring was continued for 2 h at room temperature and reaction mixture was evaporated to dryness in vacuo. The residue was dissolved in 20 mL of water and extracted (3 × 50 mL) with EtOAc. The extract was washed with 30 mL water, dried over $MgSO_4$, evaporated to dryness in vacuo to give ca. 1 g of crude product. An analytical sample was purified by PLC in the mixture of $CHCl_3$−MeOH 97:3 to yield after crystallization from MeOH 20 mg of **4g**: mp 82−85 °C; R_f (C) 0.48; ^{1}H NMR δ ($CDCl_3$) 7.22 (1H, s, H6), 6.32 (1H, dd, H1′), 5.22 (1H, m, H3′), 4.38 (1H, dd, H5″), 4.32 (1H, dd, H5′), 4.23 (1H, m, H4′), 2.43−2.38 (1H, m, H2″), 2.20−2.10 (1H, m, H2′), 2.19, 2.11 (6H, 2 × s, 2 × CH_3CO). Anal. ($C_{13}H_{16}BrN_3O_7$·0.25MeOH) C, H, N.

1-(3,5-Di-*O*-acetyl-*β*-D-2-deoxyribofuranosyl)-4-hydroxyamino-5-iodopyrimidin-2(1*H*)-one (4h). Crude nucleoside **2h** was dissolved in 20 mL of pyridine and hydroxylamine hydrochloride (150 mg, 2.16 mmol) was added. The mixture was stirred at room temperature for 12 h, evaporated under reduced pressure and coevaporated successively with 2 × 20 mL of toluene and EtOH. 50 mL of $CHCl_3$ was added and the mixture was washed with water (2 × 30 mL). The organic layer was separated, dried (Na_2SO_4) and evaporated under reduced pressure. Resulting crude **4h** was purified on a silica gel column (1 × 50 cm) with the use of $CHCl_3$ to yield 385 mg (84%) of **4h**. An analytical sample was crystallized from MeOH to yield white crystals: mp 90−92 °C; UV λ_{max} (pH 0) 305.5 nm (ϵ 9.9 × 10^3), 230 nm (ϵ 11.4 × 10^3), λ_{max} (pH 1) 293 nm (ϵ 8.05 × 10^3), 232 nm (ϵ 11.65 × 10^3), λ_{max} (pH 2) 284 nm (ϵ 7.95 × 10^3), 233 nm (ϵ 11.60 × 10^3), λ_{max} (pH 7) 284.5 nm (ϵ 8.05 × 10^3), 233 nm (ϵ 11.60 × 10^3), λ_{max} (pH 12) 247.5 nm (ϵ 11.90 × 10^3); TLC (silica gel) R_f (C) 0.45; ^{1}H NMR δ ($CDCl_3$) 7.30 (1H, s, H6), 6.30 (1H, dd, H1′), 5.23−5.20 (1H, m, H3′), 4.38 (1H, dd, H5″), 4.31 (1H, dd, H5′), 4.23 (1H, m, H4′), 2.42−2.36 (1H, m, H2″), 2.18−2.11 (1H, m, H2′), 2.22, 2.11 (6H, 2 × s, 2 × CH_3CO). Anal. ($C_{13}H_{16}IN_3O_7$·0.33MeOH) C, H, N.

General Procedure for the Deblocking and Purification of N^4-OH Nucleosides. 0.5 mmol of appropriate compound **4a**−**c**,**e**−**h** was dissolved in 15 mL of MeOH saturated at 0 °C with ammonia. The mixture was stirred at room temperature for 12 h, concentrated under reduced pressure and purified on Dowex 50W(H^+) column (0.5 × 10 cm). Product was eluted with linear gradient of water−1 N ammonia. The major UV absorbing fractions were collected and loaded on Chelex100 (H^+ form) column (0.5 × 3 cm). The product was eluted with water and concentrated under reduced pressure to give crude compounds **5a**,**b**,**d**−**h** which were purified as follows.

1-(*β*-D-2-Deoxyribofuranosyl)-4-hydroxyaminopyrimidin-2(1*H*)-one (5a).[33] Crude **5a** was crystallized from mixture of MeOH and EtOAc to yield white crystals: 98 mg (81%); mp 147−150 °C; UV λ_{max} (pH 0) 280 nm (ϵ 10.4 × 10^3), 219 nm (ϵ 6.9 × 10^3); λ_{max} (pH 1) 279.5 nm (ϵ 10.2 × 10^3), 220 nm (ϵ 7.0 × 10^3); λ_{max} (pH 2) 278.5 nm (ϵ 8.7 × 10^3), 224 nm (ϵ 6.9 × 10^3); λ_{max} (pH 7) 270 nm (ϵ 5.2 × 10^3), 234 nm (ϵ 10.0 × 10^3); λ_{max} (pH 12) 240 nm (ϵ 8.2 × 10^3); TLC (silica gel) R_f (A) 0.36; ^{1}H NMR δ (D_2O) 7.06 (1H, d, H5), 6.27 (1H, t, H1′, $J_{1'2'}$ = 7.58 Hz, $J_{1'2''}$ = 6.60 Hz), 5.74 (1H, d, H6) 4.43 (1H, m, H3′, $J_{3'4'}$ = 3.84 Hz), 3.97 (1H, m, H4′, $J_{4'5'}$ = 3.68 Hz, $J_{4'5''}$ = 5.19 Hz), 3.79 (1H, dd, H5′, $J_{5'5''}$ = −12.42 Hz), 3.72 (1H, dd, H5″), 2.33 (1H, m, H2″, $J_{2'2''}$ = −14.25 Hz, $J_{2''3'}$ = 3.63 Hz), 2.27 (1H, m, H2′, $J_{2'3'}$ = 6.98 Hz); MS *m*/*z* 244 $(M + H)^+$.

1-(*β*-D-2-Deoxyribofuranosyl)-4-hydroxyamino-5-methylpyrimidin-2(1*H*)-one (5b). Crude **5b** was crystallized from mixture of EtOAc and MeOH to yield white crystals: 110 mg (85%); mp 91−95 °C (lit.[17] 114 °C); UV λ_{max} (pH 0) 285 nm (ϵ 13.60 × 10^3), 220 nm (ϵ 9.60 × 10^3); λ_{max} (pH 1) 282.5 nm (ϵ 12.40 × 10^3), 220 nm (ϵ 9.00 × 10^3); λ_{max} (pH 2) 278 nm (ϵ 9.90 × 10^3), 224 nm (ϵ 9.40 × 10^3); λ_{max} (pH 7) 268 nm (ϵ 8.60 × 10^3), 236 nm (ϵ 11.55 × 10^3); λ_{max} (pH 12) 252 nm (ϵ 10.80 × 10^3); TLC (silica gel) R_f (A) 0.49; ^{1}H NMR δ (D_2O) 6.96 (1H, s, H6), 6.28 (1H, t, H1′, $J_{1'2'}$ = 7.54 Hz, $J_{1'2''}$ = 6.58 Hz), 4.44 (1H, m, H3′, $J_{3'4'}$ = 3.99 Hz, $J_{3'2'}$ = 6.89 Hz, $J_{3'2''}$ = 3.70 Hz), 3.97 (1H, m, H4′, $J_{4'5'}$ = 3.99 Hz, $J_{4'5''}$ = 5.02 Hz), 3.81 (1H, dd, H5′, $J_{5'5''}$ = −12.41 Hz), 3.74 (1H, dd, H5″), 2.34 (1H, m, H2″), 2.27 (1H, m, H2′, $J_{2'2''}$ = −14.25 Hz), 1.81 (3H, s, 5-CH_3); MS *m*/*z* 258 $(M + H)^+$.

1-(*β*-D-2-Deoxyribofuranosyl)-4-hydroxyamino-5-hydroxymethylpyrimidin-2(1*H*)-one (5d). Crude **5d** was crystallized from mixture of toluene and MeOH to yield white crystals: 127 mg (93%); mp 188−190 °C dec; UV λ_{max} (pH 0) 281.5 nm (ϵ 14.20 × 10^3), 219 (ϵ 12.40 × 10^3); λ_{max} (pH 1) 281.5 nm (ϵ 9.60 × 10^3), 224.5 nm (ϵ 8.80 × 10^3); λ_{max} (pH 2) 275 nm (ϵ 7.60 × 10^3), 230 nm (ϵ 12.10 × 10^3); λ_{max} (pH 7) 274 nm (ϵ 6.90 × 10^3), 231.5 nm (ϵ 12.75 × 10^3); λ_{max} (pH 12) 251 nm (ϵ 10.60 × 10^3); TLC (silica gel) R_f (A) 0.25; ^{1}H NMR δ (D_2O) 7.14 (1H, s, H6), 6.30 (1H, t, H1′, $J_{1'2'}$ = 7.44 Hz $J_{1'2''}$ = 6.63 Hz), 4.46 (1H, m, H3′, $J_{3'4'}$ = 3.70 Hz, $J_{3'2'}$ = 6.79 Hz, $J_{3'2''}$ = 3.80 Hz), 4.29 (2H, d, 5-CH_2OH), 3.99 (1H, m, H4′, $J_{4'5'}$ = 3.53 Hz, $J_{4'5''}$ = 5.07 Hz), 3.83 (1H, dd, H5′, $J_{5'5''}$ = −12.43 Hz), 3.76 (1H, dd, H5″), 2.36 (1H, m, H2″), 2.30 (1H, m, H2′, $J_{2'2''}$ = −14.14 Hz); MS *m*/*z* 274.10151 [$(M + H)^+$ calcd for $C_{10}H_{16}N_3O_6$ 274.10391]. Anal. ($C_{10}H_{15}N_3O_6$) C, H, N.

1-(*β*-D-2-Deoxyribofuranosyl)-4-hydroxyamino-5-fluoropyrimidin-2(1*H*)-one (5e).[18] Title compound was obtained as a glass: 115 mg (88%); mp 94−97 °C; UV λ_{max} (pH 0) 286 nm (ϵ 14.6 × 10^3), 222 nm (ϵ 10.6 × 10^3), λ_{max} (pH 7) 270 nm (ϵ 10.4 × 10^3), 234 nm (ϵ 13.3 × 10^3), λ_{max} (pH 12) 253 nm (ϵ 13.5 × 10^3); TLC (silica gel) R_f (A) 0.44; ^{1}H NMR δ (D_2O) 7.34 (1H, d, H6) 6.32 (1H, td, H1′), 4.47 (1H, m, H3′, $J_{2'3'}$ = 5.14 Hz, $J_{2''3'}$ = 5.14 Hz), 4.02 (1H, m, H4′, $J_{4'3'}$ = 3.65 Hz), 3.85 (1H, dd, H5′, $J_{4'5'}$ = 3.65 Hz), 3.78 (1H, dd, H5″, $J_{4'5''}$ = 4.91

Hz) 2.33 (2H, dd, H2′, H2″, $J_{1'2'}+J_{1'2''}/2$ = 6,96 Hz,); MS *m/z* 262 $(M + H)^+$.

1-(β-D-2-Deoxyribofuranosyl)-4-hydroxyamino-5-chloropyrimidin-2(1*H*)-one (5f). The product **5f** was obtained as an amorphous foam: 120 mg (87%); mp 92−95 °C; UV λ_{max} (pH 0) 294 nm (ϵ 15.3 × 10^3), 226 nm (ϵ 11.95 × 10^3); λ_{max} (pH 1) 288 nm (ϵ 10.8 × 10^3), 226 nm (ϵ 12.45 × 10^3); λ_{max} (pH 2) 282 nm (ϵ 10.2 × 10^3), 233 nm (ϵ 13.2 × 10^3); λ_{max} (pH 7) 281 nm (ϵ 10.1 × 10^3), 234 nm (ϵ 13.8 × 10^3); λ_{max} (pH 12) 284 nm (ϵ 9.4 × 10^3), 250 nm (ϵ 1.42 × 10^3); TLC (silica gel) R_f (A) 0.54; ^{1}H NMR δ [ppm] (D_2O) 7.40 (1H, s, H6), 6.25 (1H, t, H1′, $J_{1'2'}$ = 6.95 Hz, $J_{1'2''}$ = 6.74 Hz), 4.44 (1H, m, H3′, $J_{3'4'}$ = 4.14 Hz), 3.98 (1H, m, H4′), 3.81 (1H, dd, H5′, $J_{4'5'}$ = 4.02 Hz), 3.74 (1H, dd, H5″, $J_{4'5''}$ = 4.47 Hz, $J_{5'5''}$ = −12.46 Hz), 2.32 (1H, m, H2″, $J_{2'2''}$ = −14.21 Hz, $J_{2''3'}$ = 3.42 Hz), 2.30 (1H, m, H2′, $J_{2'3'}$ = 7.32 Hz). Anal. ($C_9H_{12}ClN_3O_5$) C, H, N.

1-(β-D-2-Deoxyribofuranosyl)-4-hydroxyamino-5-bromopyrimidin-2(1*H*)-one (5g). Crude **5g** was crystallized from MeOH to yield white crystals: 500 mg (67%); mp 187−190 °C dec; UV λ_{max} (pH 0) 297 nm (ϵ 11.35 × 10^3), 225 nm (ϵ 9.00 × 10^3); λ_{max} (pH 1) 291 nm (ϵ 8.75 × 10^3), 229 nm (ϵ 10 × 10^3); λ_{max} (pH 2) 283 nm (ϵ 7.80 × 10^3), 231 nm (ϵ 10.80 × 10^3); λ_{max} (pH 7) 282 nm (ϵ 7.80 × 10^3), 231 nm (ϵ 11.05 × 10^3); λ_{max} (pH 12) 282 nm (ϵ 6.70 × 10^3), 245 nm (ϵ 10.30 × 10^3); TLC (silica gel) R_f (A) 0.54; ^{1}H NMR δ (D_2O) 7.49 (1H, s, H6), 6.25 (1H, dd, H1′, $J_{1'2'}$ = 6.90 Hz, $J_{1'2''}$ = 6.68 Hz), 4.44 (1H, m, H3′, $J_{2'3'}$ = 7.12 Hz), 3.98 (1H, m, H4′, $J_{3'4'}$ = 3.96 Hz), 3.81 (1H, dd, H5′, $J_{4'5'}$ = 3.73 Hz, $J_{5'5''}$ = −12.44), 3.74 (1H, dd, H5″$J_{4'5''}$ = 4.82 Hz), 2.33 (1H, m, H2″, $J_{2''3'}$ = 3.73 Hz), 2.30 (1H, m, H2′, $J_{2'2''}$ = −14.22 Hz). Anal. ($C_9H_{12}BrN_3O_5$) C, H, N.

1-(β-D-2-Deoxyribofuranosyl)-4-hydroxyamino-5-iodopyrimidin-2(1*H*)-one (5h). Crude **5h** after crystallization from MeOH yield white crystals: 146 mg (79%); mp 181−184 °C dec; UV λ_{max} (pH 0) 305.5 nm (ϵ 9.9 × 10^3) 230 nm (ϵ 11.4 × 10^3); λ_{max} (pH 1) 293 nm (ϵ 8.05 × 10^3), 232 nm (ϵ 11.65 × 10^3); λ_{max} (pH 2) 284 nm (ϵ 7.95 × 10^3), 233 nm (ϵ 11.60 × 10^3); λ_{max} (pH 7) 284.5 nm (ϵ 8.05 × 10^3), 233 nm (ϵ 11.60 × 10^3); λ_{max} (pH 12) 247.5 nm (ϵ 11.90 × 10^3); TLC (silica gel) R_f (A) 0.59; ^{1}H NMR (D_2O) 7.56 (1H, s, H6), 6.22 (1H, t, H1′, $J_{1',2'}$ = 6.87 Hz, $J_{1',2''}$ = 6.71 Hz), 4.44 (1H, m, H3′, $J_{3'4'}$ = 4.00 Hz), 3.97 (1H, m, H4′, $J_{4',5'}$ = 3.53 Hz, $J_{4'5''}$ = 4.75 Hz), 3.82 (1H, dd, H5′, $J_{5'5''}$ = −12.55 Hz), 3.75 (1H, m, H5″), 2.34 (1H, m, H2″, $J_{2'2''}$ = −14.25 Hz, $J_{2''3'}$ = 3.98 Hz), 2.30 (1H, m, H2′, $J_{2'3'}$ = 6.81 Hz). Anal. ($C_9H_{12}IN_3O_5$·0.33 MeOH) C, H, N.

General Procedure for the Synthesis of Nucleoside 5′-Phosphates. To a solution of 0.05 mmol of the appropriate nucleoside analogue **5a**,**b**,**d**−**h** in 1.5 mL of 0.1 M acetate buffer pH 4 was added 280 mg (0.75 mmol) of *p*-nitrophenyl phosphate and the pH was brought to 4 by addition of concentrated acetic acid. To this was added 1.5 mL of a crude extract of wheat shoot nucleoside phosphotransferase. The mixture was incubated at 37 °C for 40 h, concentrated to half-volume and extracted 3 times with ether. After evaporation of the aqueous layer the product was purified by column chromatography on a DEAE-Sephadex A-25 eluted with a linear gradient of aqueous $Et_3N-H_2CO_3$ (0−0.5 M). The homogeneous fractions containing pure monophosphate were pooled and lyophilized to remove excess bicarbonate buffer to yield the appropriate nucleoside 5′-monophosphates **6a**,**b**,**d**−**h** as triethylammonium salts. UV spectra of nucleotides **6a,b,d**−**h** were almost identical to spectra of their mother nucleosides **5a**,**b**,**d**−**h** (see below).

General Procedure for the Enzymatic Hydrolysis of Nucleoside 5′-Phosphates. To a solution of 40 μL 0.1 M Tris/HCl buffer pH 8.8 + 20 μL 0.1 M $MgCl_2$ was added 0.05 μmol of nucleoside 5′-phosphate, followed by 5 μL of a 10 mg/mL stock solution of *Crotalus adamanteus* (EC 3.1.3.5.) snake venom phosphodiesterase (5′-nucleotidase). Following 2 h incubation at 37 °C, nucleoside 5′-monophosphates **6a**,**b**,**d**−**h** underwent ∼50% hydrolysis to their mother nucleosides **5a**,**b**,**d**−**h** while the "natural" substrate dCMP was quantitatively converted to the parent nucleoside dCyd. After overnight incubation at 37 °C all nucleotides were quantitatively hydrolyzed to their mother nucleosides. An additional control, 2′-(3′)-GMP was unaffected, pointing to the absence of nonspecific phosphatases.

1-(β-D-2-Deoxyribofuranosyl)-4-hydroxyaminopyrimidin-2(1*H*)-one 5′-monophosphate (6a): 18 mg (70%); UV λ_{max} (pH 0) 278 nm (ϵ 10.30 × 10^3), 218 nm (ϵ 6.83 × 10^3); λ_{max} (pH 7) 271 nm (ϵ 5.15 × 10^3), 234 nm (ϵ 9.99 × 10^3); λ_{max} (pH 12) 241 nm (ϵ 8.12 × 10^3); TLC (cellulose) R_f (D) 0.49, (E) 0.30, (F) 0.42; P/ϵ 1.00.

1-(β-D-2-Deoxyribofuranosyl)-4-hydroxyamino-5-methylpyrimidin-2(1*H*)-one 5′-monophosphate (6b): 18.3 mg (68%); UV λ_{max} (pH 0) 283 nm (ϵ 13.70 × 10^3), 219 nm (ϵ 9.50 × 10^3); λ_{max} (pH 7) 269 nm (ϵ 8.51 × 10^3), 236 nm (ϵ 11.67 × 10^3); λ_{max} (pH 12) 253 nm (ϵ 10.69 × 10^3); TLC (cellulose) R_f (D) 0.46, (E) 0.32, (F) 0.42; P/ϵ 1.01.

1-(β-D-2-Deoxyribofuranosyl)-4-hydroxyamino-5-hydroxymethylpyrimidin-2(1*H*)-one 5′-monophosphate (6d): 15.8 mg (57%); UV λ_{max} (pH 0) 280 nm (ϵ 14.00 × 10^3), 218 (ϵ 12.30 × 10^3); λ_{max} (pH 7) 275 nm (ϵ 6.83 × 10^3), 231 nm (ϵ 12.63 × 10^3); λ_{max} (pH 12) 252 nm (ϵ 10.50 × 10^3); TLC (cellulose) R_f (D) 0.41, (E) 0.27, (F) 0.27; P/ϵ 1.02.

1-(β-D-2-Deoxyribofuranosyl)-4-hydroxyamino-5-fluoropyrimidin-2(1*H*)-one 5′-monophosphate (6e): 16.8 mg (62%); UV λ_{max} (pH 0) 282 nm (ϵ 14.5 × 10^3), 223 nm (ϵ 10.5 × 10^3), λ_{max} (pH 7) 269 nm (ϵ 10.3 × 10^3), 234 nm (ϵ 13.2 × 10^3), λ_{max} (pH 12) 254 nm (ϵ 13.4 × 10^3); TLC (cellulose) R_f (D) 0.44, (E) 0.28, (F) 0.41; P/ϵ 1.01.

1-(β-D-2-Deoxyribofuranosyl)-4-hydroxyamino-5-chloropyrimidin-2(1*H*)-one 5′-monophosphate (6f): 14 mg (50%); UV λ_{max} (pH 0) 293 nm (ϵ 15.2 × 10^3), 225 nm (ϵ 11.80 × 10^3); λ_{max} (pH 7) 282 nm (ϵ 10.0 × 10^3), 234 nm (ϵ 13.7 × 10^3); λ_{max} (pH 12) 285 nm (ϵ 9.3 × 10^3), 250 nm (ϵ 1.30 × 10^3); TLC (cellulose) R_f (D) 0.46, (E) 0.30, (F) 0.27; P/ϵ 1.00.

1-(β-D-2-Deoxyribofuranosyl)-4-hydroxyamino-5-bromopyrimidin-2(1*H*)-one 5′-monophosphate (6g): 17.5 mg (58%); UV λ_{max} (pH 0) 295 nm (ϵ 11.20 × 10^3), 224 nm (ϵ 8.90 × 10^3); λ_{max} (pH 7) 283 nm (ϵ 7.70 × 10^3), 231 nm (ϵ 10.90 × 10^3); λ_{max} (pH 12) 283 nm (ϵ 6.60 × 10^3), 246 nm (ϵ 10.20 × 10^3); TLC (cellulose) R_f (D) 0.48, (E) 0.28, (F) 0.29; P/ϵ 1.01.

1-(β-D-2-Deoxyribofuranosyl)-4-hydroxyamino-5-iodopyrimidin-2(1*H*)-one 5′-monophosphate (6h): 19.5 mg (60%); UV λ_{max} (pH 0) 304 nm (ϵ 9.8 × 10^3) 229 nm (ϵ 11.3 × 10^3); λ_{max} (pH 7) 285 nm (ϵ 7.97 × 10^3), 233 nm (ϵ 11.50 × 10^3); λ_{max} (pH 12) 248 nm (ϵ 11.80 × 10^3); TLC (cellulose) R_f (D) 0.46, (E) 0.29, (F) 0.27; P/ϵ 1.00.

Acknowledgment. This work was supported by the Polish State Committee for Scientific Research, Grants 4P05F03011p01 and 4P05F03011p02.

References

(1) Carreras, C. W.; Santi, D. V. The Catalytic Mechanism and Structure of Thymidylate Synthase. *Annu. Rev. Biochem.* **1995**, *64*, 721−762.
(2) Rode, W.; Leś, A. Molecular Mechanism of Thymidylate Synthase-catalyzed Reaction and Interaction of the Enzyme with 2- and/or 4-substituted Analogues of dUMP and 5-Fluoro-dUMP. *Acta Biochim. Pol.* **1996**, *43*, 133−142.
(3) Danenberg, P. V. Thymidylate Synthetase − a Target Enzyme in Cancer Chemotherapy. *Biochim. Biophys. Acta* **1977**, *473*, 73−92.
(4) Heidelbereger, C.; Danenberg, P. V.; Moran, R. G. Fluorinated Pyrimidines and Their Nucleosides. *Adv. Enzymol.* **1983**, *54*, 57−119.
(5) Jackman, A. L.; Jones, T. R.; Calvert, A. H. Thymidylate Synthetase Inhibitors: Experimental and Clinical Aspects. In *Experimental and Clinical Progress in Cancer Chemotherapy*; Muggia, F. M., Ed.; Martinus Nijhoff Publishers: Boston, 1985; pp 155−210.
(6) Ealick, S. E.; Armstromg, S. R. Pharmacologically Relevant Proteins. *Curr. Opin. Struct. Biol.* **1993**, *3*, 861−867.
(7) Santi, D. V. Perspectives on the Design and Biochemical Pharmacology of Inhibitors of Thymidylate Synthetase. *J. Med. Chem.* **1980**, *23*, 103−111.

(8) Lewis, C. A., Jr.; Dunlap, R. B. Thymidylate Synthase and its Interaction with 5-Fluoro-2′-deoxyuridylate. In *Topics in Molecular Pharmacology*; Burgen, A. S. V., Roberts, G. C. K., Eds.; Elsevier/North-Holland Biomedical: New York, 1981; pp 170−219.
(9) De Clercq, E.; Balzarini, J.; Torrence, P. F.; Mertes, M. P.; Schmidt, C. L.; Shugar, D.; Barr, P. J.; Jones, A. S.; Verhelst, G.; Walker, R. T. Thymidylate Synthetase As Target Enzyme for the Inhibitory Activity of 5-substituted 2′-deoxyuridines on Mouse Leukemia L1210 Cell Growth. *Mol. Pharmacol.* **1981**, *19*, 321−330.
(10) Lorenson, M. Y.; Maley, G. F.; Maley, F. The Purification and Properties of Thymidylate Synthetase From Chick Embryo Extracts. *J. Biol. Chem.* **1967**, *242*, 3332−3344.
(11) Goldstein, S.; Pogolotti, A. L.; Garvey, Jr.; E. P.; Santi, D. V. Interaction of N^4-hydroxy-2′-deoxycytidylic Acid with Thymidylate Synthetase. *J. Med. Chem.* **1984**, *27*, 1259−1262.
(12) Rode, W.; Zieliński, Z.; Dzik, J. M.; Kulikowski, T.; Bretner M.; Kierdaszuk B.; Cieśla, J.; Shugar D. Mechanism of Inhibition of Mammalian Tumor and Other Thymidylate Synthases by N^4-hydroxy-dCMP, N^4-hydroxy-5-fluoro-dCMP, and Related Analogues. *Biochemistry* **1990**, *29*, 10835−10842.
(13) Brown, D. M.; Shell, P. The Reaction of Hydroxylamine with Cytosine and Related Compounds. *J. Mol. Biol.* **1961**, *3*, 709−710.
(14) Brown, D. M.; Shell, P. Nucleosides Part XLVIII. The Reaction of hydroxylamine with Cytosine and Related Compounds. *J. Chem. Soc.* **1965**, 208−215.
(15) Maley, G. F.; Maley, F. The Purification and Properties of Deoxycytidylate Deaminase From Chick Embryo Extracts. *J. Biol. Chem.* **1964**, *239*, 1168−1176.
(16) Janion, C.; Shugar, D. Studies on Possible Mechanisms of Hydroxylamine Mutagenesis. *Acta Biochim. Polon.* **1968**, *15*, 107−121.
(17) Fox, J. J.; Van Praag, D.; Wempen, I.; Doerr, I. L.; Cheong, L.; Knoll, J. E.; Eidinoff, M. L.; Bendich, A.; Brown, G. B. Thiation of Nucleosides. II. Synthesis of 5-Methyl-2′-deoxycytidine and Related Pyrimidine Nucleosides. *J. Am. Chem. Soc.* **1959**, *81*, 178−187.
(18) Wempen, I.; Miller, N.; Falco, E. A.; Fox, J. J. Nucleosides. XLVII. Syntheses of Some N^4-substituted Derivatives of 1-β-D-arabinofuranosylcytosine and −5-Fluorocytosine. *J. Med. Chem.* **1968**, *11*, 144−148.
(19) Mertes, M. P.; Smrt, J. Nucleic Acid Components and Their Analogues. CXV. Synthesis of N^4-Hydroxy-6-azacytidine 5′-Phosphate and 5′-Diphosphate. *Collect. Czech. Chem. Commun.* **1968**, *33*, 3304−3312.
(20) Herdewijn, P.; Balzarini, J.; Baba, M.; Pauwels, R.; Janssen, G.; De Clercq, E. Synthesis and Anti HIV Activity of Different Sugar Modified Pyrimidine and Purine Nucleosides. *J. Med. Chem.* **1988**, *31*, 2040−2048.
(21) Robins, M. J.; Barr, P. J.; Giziewicz, J. Nucleic Acid Related Compounds. 38. Smooth and High-yield Iodination and Chlorination at C-5 of Uracil Bases and p-Tolyl-Protected Nucleosides. *Can. J. Chem.* **1982**, *60*, 554−557.
(22) Asakura, J.; Robins, M. J. Cerium (IV)-Mediated Halogenation at C-5 of Uracil Derivatives. *J. Org. Chem.* **1990**, *55*, 4928−4933.
(23) Robins, M. J.; MacCoss, M.; Naik, S. R,; Ramani, G. Nucleic Acid Related Compounds. 21. Direct Fluorination of Uracil and Cytosine Bases and Nucleosides Using Trifluoromethyl Hypofluorite. Mechanism, Stereochemistry, and Synthetic Applications. *J. Am. Chem. Soc.* **1976**, *98*, 7381−7390.
(24) Divakar, K. J.; Reese, C. B. 4-(1,2,4-Triazol-1-yl)- and 4-(3-Nitro-1,2,4-triazol-1-yl)-1-(β-D-2,3,5-tri-O-acetylarabinofuranosyl)pyrimidin-2(1H)-ones. Valuable Intermediates in the Synthesis of Derivatives of 1-(β-D-Arabinofuranosyl)cytosine (Ara-C). *J. Chem. Soc., Perkin Trans. 1* **1982**, 1171−1176.
(25) Matsuda, A.; Obi, K.; Miyasaka, T. Reaction of Uracil Nucleosides with 1-Methylimidazole in the Presence of Phosphoryl Chloride. A Convenient Method for the Synthesis of 4-Substituted Pyrimidin-2(1H)-one. Nucleosides. *Chem. Pharm. Bull.* **1985**, *33*, 2575−2578.
(26) Giziewicz, J.; Shugar, D. Enzymatic Phosphorylation of Nucleosides to the 5′-phosphates. In *Nucleic Acid Chemistry*; Townsend, L. B., Tipson, R. S., Eds.; John Wiley: New York, 1985; pp 955−961.
(27) Clark, M.; Cramer, R. D.; Van Opdenbosh, N. Validation of the General Purpose Tripos 5.2 Force Field. *J. Comput. Chem.* **1989**, *10*, 982−1012.
(28) Leś, A.; Adamowicz, L.; Rode, W. Structure and Conformation of N^4-hydroxycytosine and N^4-hydroxy-5-fluorocytosine. A Theoretical Ab Initio Study. *Biochim. Biophys. Acta* **1993**, *1173*, 39−48.
(29) Gunther, H. *NMR Spectroscopy. An Introduction;* John Wiley and Sons: Chichester, 1980; pp 125−140.
(30) Remin, M. Thermodynamic cycle between DNA and RNA Constituents for Conformation of the Sugar Ring from Nuclear Magnetic Resonance Study. *J. Biomol. Struct. Dyn.* **1997**, *15*, 251−264.
(31) De Leeuw, F.A. A. M.; Altona, C. Conformation Analysis of β-D-Ribo, β-D-Deoxyribo, β-D-Arabino, β-D-Xylo, β-D-Lyxo-nucleosides from Proton−Proton Coupling Constant. *J. Chem. Soc., Perkin Trans. 2* **1982**, 375−384.
(32) Garret, C.; Wataya, Y.; Santi, D. V. Thymidylate Synthase. Catalysis of Dehalogenation of 5-bromo- and 5-iodo-2′-deoxyuridylate. *J. Med. Chem.* **1979**, *13*, 2798−2804.
(33) Nelson, D. J.; Carter, C. E. Inhibition of the Biosynthesis of Thymidylic Acid by 4-N-hydroxy-2′-deoxycytidine in L5178Y Leukemic Cells. *Mol. Pharmacol.* **1966**, *2*, 248−258.
(34) Dollinger, M. R.; Burchenal, J.h.; Kreis, W.; Fox, J. J. Analogues of 1-β-D-arabinofuranosylcytosine. Studies on Mechanisms of Action in Burkitt's Cell Culture and Mouse Leukemia, and in vitro Deamination Studies. *Biochem. Pharmacol.* **1967**, *16*, 689−706.
(35) Leś, A.; Adamowicz, L.; Rode, W. Modelling of Reaction Steps Relevant to Deoxyuridylate (dUMP) Enzymatic Methylation and Thymidylate Synthase Mechanism-based Inhibition. *J. Biomol. Struct. Dyn.* **1998**, *15*, 703−715.
(36) Wataya, Y.; Santi, D. V. Inhibition of *Loctobacillus casei* Thymidylate Synthetase by 5-Substituted 2′-Deoxyuridylates. Preliminary Quantitative Structure−Activity Relationship. *J. Med. Chem.* **1977**, *20*, 1469−1473.
(37) Chen, P. S., Jr.; Toribara, T. Y.; Warner, H. Microdetermination of Phosphorus. *Anal. Chem.* **1956**, *28*, 1756−1758.
(38) Dzik, J. M.; Bretner, M.; Kulikowski, T.; Gołos, B.; Jarmuła, A.; Poznański, J.; Rode, W.; Shugar, D. Synthesis and Interactions with Thymidylate Synthase of 2,4-dithio- Analogues of dUMP and 5-fluoro-dUMP. *Biochim. Biophys. Acta* **1996**, *1293*, 1−8.
(39) Zieliński, Z.; Dzik, J. M.; Rode, W.; Kulikowski, T.; Bretner, M.; Kierdaszuk, B.; Shugar, D. Interaction of N^4-hydroxy-dCMP and N^4-hydroxy-5-FdCMP with L1210 Thymidylate Synthase Differing in Sensitivity Towards 5-FdUMP Inhibition. In *Chemistry and Biology of Pteridines 1989. Pteridines and Folic Acid Derivatives*; Curtius, H.-Ch., Ghisla, S., Blau, N., Eds.; Walter de Gruyter: Berlin, 1990; pp 817−820.
(40) Cieśla, J.; Weiner, K. X. B.; Weiner, R. S.; Reston, J. T.; Maley, G. F.; Maley, F. Isolation and Expression of Rat Thymidylate Synthase cDNA: Phylogenetic Comparison with Human and Mouse Thymidylate Synthases. *Biochim. Biophys. Acta* **1995**, *1261*, 233−242.
(41) Dąbrowska, M.; Zieliński, Z.; Wranicz, M.; Michalski, R.; Pawełczak, K.; Rode, W. *Trichinella Spiralis* Thymidylate Synthase: Developmental Pattern, Isolation, Molecular Properties and Inhibition by Substrate and Cofactor Analogues. *Biochem. Biophys. Res. Commun.* **1996**, *228*, 440−445.
(42) Brouillette, C. B.; Chang, C. T.-C.; Mertes, M. P. 5-(α-Bromoacetyl)-2′-Deoxyuridine 5′-phosphate: An Affinity Label for Thymidylate Synthetase. *J. Med. Chem.* **1979**, *22*, 1541−1544.
(43) Tanty, C. R.; Lopez-Canovas, L.; Brauet, A. L.; Paredes, M. R.; Clarke, D. H.; Castro, H. V.; Rojas, A. M. R.; Cabrera, A. M. Introduction of an Immunochemical Label in a Cytidine Analogue. *Nucleosides Nucleotides* **1995**, *14*, 219−228.
(44) Poznański, J.; Felczak, K.; Kulikowski, T.; Remin, M. ^{1}H NMR Conformational Study of Antiherpetic C5−Substituted 2′-Deoxyuridines: Insight into the Nature of Structure−Activity Relationships. *Biochem. Biophys. Res. Commun.* **2000**, *272*, 64−74.

JM000975U